Numerical Investigation of Dynamic Stall for Non-Stationary Two-Dimensional Blade Airfoils

G.S.T.A. Bangga[1*], H. Sasongko[2]

[1,2]Department of mechanical engineering
Field of study energy conversion
Institut Teknologi Sepuluh Nopember (ITS), Surabaya, Indonesia
*Corresponding author : probability.schrodinger@gmail.com

Abstract

In the analysis of the helicopter blades, turbo-machinery compressor blades, wind turbines and other streamlined structures operating at high angle of incidence, the necessity and importance of including an non-stationary effect of the local two-dimensional flow, the so-called dynamic stall becomes increasingly important. It could affect performance and also reduce fatigue life of many modern lightweight blades through the induced vibrations. The event of the dynamic stall occurred on the suction side of airfoils that are shown by dynamic lift exceeds maximum static lift at the static stall angle. Numerical methods using two turbulence URANS model, namely *standard-kω* and*SST-kω*, is used in the analysis to investigate the dynamics induced by the present model on a two-dimensional airfoil and also to explain physics of these phenomenon.It is demonstrated that the *SST-kω* performs better than *standard-kω* to predict hysteresis lift coefficient. The onset of travelling vortex phenomenon could be well captured. The intended applications of this paper lie in the field of unsteady rotary-wing aerodynamics and its characteristics on the induced vibration.

Keywords: Dynamic stall, Non-stationary two dimensional airfoils, CFD, External flows

Introduction

The term dynamic stall usually refers to an unsteady flow characterized by the formation, convection and shedding of a vortex on the suction side of an airofoil [1]. The event of the dynamic stall on the aerodynamic bodies involve complex separated flow and even in the transition zone. The occurrence of dynamic stall is caused by the high aeroelasticity on the airfoil at high angle of attack. Unlike the static stall, the stall on the dynamic conditions can be delayed on airfoil with angle of attack increases rapidly and even beyond the critical static stall angle of attack significantly. However, when dynamic stall occurs, the aerodynamic loads generally larger than the static stall and lead to increased stress acting on the airfoil significantly and potentially harmful the airfoil structure itself [2]. Dynamic stall events initiated by the leading edge separation, leading edge vortex developed and moves downstream along the airfoil surface. Vortex reaches the trailing edge and dettach followed by a trailing edge vortex formation and indicate the onset of stall. The detachment of the trailing edge vortex occurs as the increase in angle of attack followed by a leading edge vortex breakdown. These events resulted in a drastic decrease in lift coefficient and the flow reattachment will occur at fairly low angle of attack again. Figure 1 shows the event of stall at the dynamic conditions by CFD calculation on the NACA 0015 [3]. Fig. 1(a) illustrates the onset of leading edge separation with the entire boundary layer starting to detach. Fig. 1(b) shows the build-up of the leading edge vortex, which in Fig. 1(c) detaches and moves downstream, while a trailing edge vortex starts building up. Finally, Fig. 1(d) shows the detachment of the trailing edge vortex and breakdown of the leading edge travelling vortex. Both experimental data and CFD calculations indicate that the flow changes, caused by the leading edge separation vortex,generate an increased suction contribution, leading to an increased lift even after flow separation has occurred [3]. This effect may be seen in figure 2 as the dynamic curve that continues to increase above the static stall angle.

Since the first analysis on aircraft aeroelasticity, unsteady aerodynamic airfoil studied experimentally and theoretically. Dynamic stall, until the 1950's only studied experimentally, in the late 1970's a new mathematical model of dynamic stall was introduced by Friedmann and since then the modeling of dynamic stall developed [6]. Mathematical modeling of dynamic stall lot to do ranging from simple to complex, including the ONERA [7], Boeing [8], Johnson [9], ø ye [10], Ris ø [6] and also Leishman-Beddoes model [11, 12]. Meyer, et al. [13] modeled the dynamic stall based on the DLR models by utilizing the state-space representation. This involves modeling of the instationary effects using solution of Theodorsen equation in the time domain called Wagner function and Küssner function. These two functions describe the dynamic stall hysteresis curve in the linear zone. Based on the verification, this modified numerical ODE method produces dynamic stall plot corresponding to the occuring physical phenomena. However, the mathematical formulation of the model is difficult to trace DLR physically because of the mathematical formalism that is used not accompanied by a translation of the differential analysis. Dynamic stall on wind turbine models are developed by JW Larsen, et al. [3] with a backbone models based on the static lift curve. Modeling of the static lift is described by two parameters, at fully attached flow and lift depending on the degree of attachment. This mathematical modeling used the data obtained from the inviscid static stall lift and is corrected using a viscous separation factor on a flat plate approach based on Kirchhoff's potential flow theory. Based on data obtained static stall, the effects of instationary dynamic stall will be involved by using the solution of convolution integral on the impulse response function. CFD analysis for the dynamic stall at low Reynolds number was developed by Wang [14] to simulate the NACA 0012 oscillating airfoil. This study used two turbulence modeling, using *Standard-kω* and *SST-kω* and revealed that the used of *SST-kω*give more accurate result better *Standard-kω*models. Therefore, the objective of this paper is toassess the ability of the *Standard-kω* model and the *SST-kω* model to correctly simulate dynamic stall on the two dimensional Boeing-Vertol V23010-1.58 rotorcraft airfoil which is found in the wind turbines and make a contribution towards a better understanding of the flow physics of dynamic stall in order to assist in the design optimizations of wind turbines intended for the built and urban environment in the future.

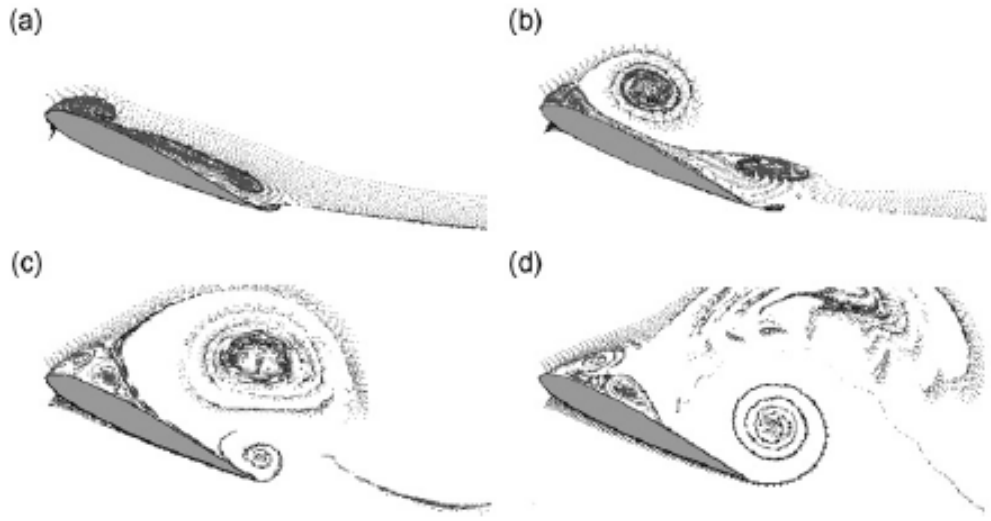

Figure 1. Flow visualisation of a CFD calculation performed on a NACA-0015 wing section during dynamic stall conditions. (a) Leading edge separation starts. (b) Vortex build-up at the leading edge. (c) Detachment of leading edge vortex and build-up of trailing edge vortex. (d) Detachment of trailing edge vortex and breakdown of leading edge vortex [4].

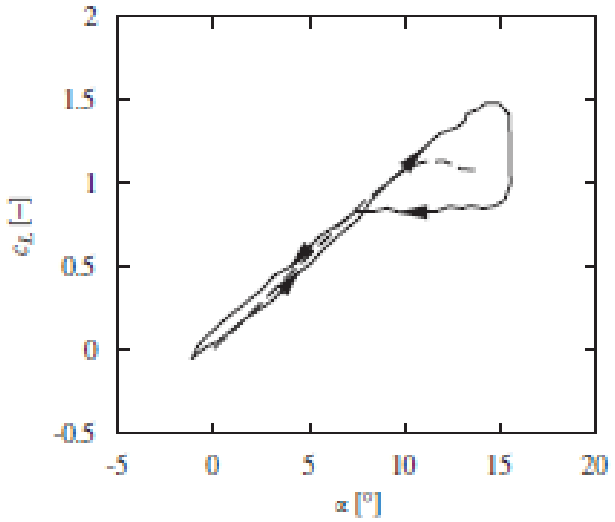

Figure 2. Lift coefficient under static and dynamic stall situations:
– –, static lift; —, dynamic lift [5]

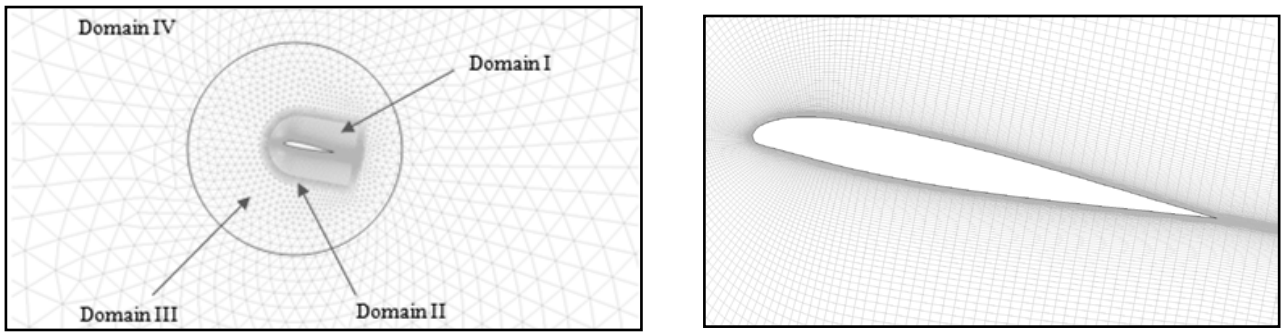

(a) (b)

Figure 3. Diagram of the sub-grid structure: (a) domain classification and (b) meshing near airfoil.

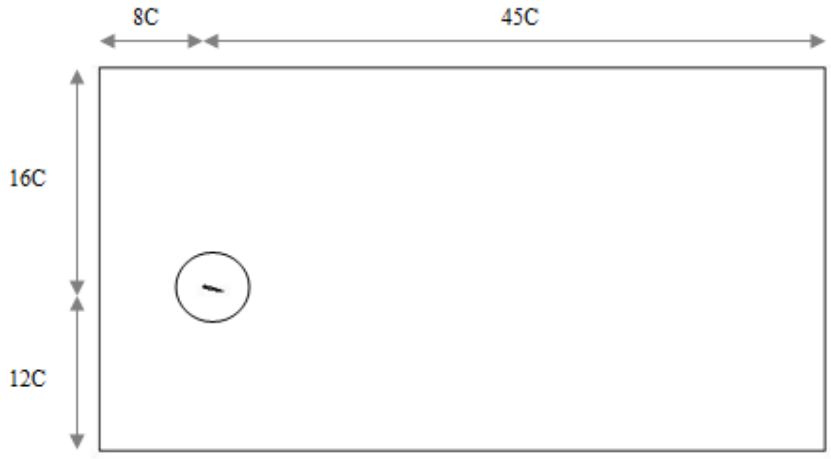

Figure 4. Domain of the analysis.

Numerical Method

Turbulence simulation methods are generally divided into three main forms, namely the Direct Numerical Simulation (DNS), Large Eddy Simulation (LES) and Unsteady Reynolds-averaged Navier-Stokes (URANS) [14]. DNS as the most advanced computational methods in solving both space and time scales require high computing technology so that the use of this method would require a high computational cost when applied to the case in this study. The use of LES will also require high computing technology to be applied to the phenomenon of dynamic stall and 3D simulation should be performed due to the nature of the eddy in 3D. URANS is a suitable method of dynamic stall approach with low computational cost and acceptable accuracy, therefore URANS would be used in this present study. Although the dynamic stall flow studied here is inherently a 3D phenomenon,

measurements have been taken to ensure a 2D flow in the mid-span plane, where the experimental data were obtained, in the case investigated. Thus, in the present simulations, 2D geometrical configurations are employed to model the experimental investigations and a 2D incompressible unsteady CFD solver, based on the finite volume method in the commercial software package Fluent, is employed to solve the full URANS governing equations.Due to the incompressibility of the flow studied, the pressure-based solver, which employs an algorithm which belongs to the so-called ‘‘projection method” and is traditionally implemented to solve low-speed incompressible flows, is chosen [14]. All the governing equations for the solution variables, which are decoupled from each other, are solved sequentially and the SIMPLE algorithm is applied as the pressure-velocity coupling algorithm. With respect to the discretization of the convection terms in the transport equations for the velocity and the turbulence quantities, second-order upwind schemes are utilised [14]. In order to simulate the sinusoidal pitching motion of the blade, the dynamic-mesh technique is employed. As seen on the figure 3, the hybrid mesh [15] domain were divided into four sub-domain with , domain 1 contains fine mesh and region 2 to region 4 contains coarser mesh. Corresponding to the pitching motion of the blade in reality, the blade geometry with domain 1, 2, and 3 pitches like a rigid body with the sinusoidal mode, $\alpha = \alpha_0 + \alpha_l \cos \omega t$, as the blade with $\alpha_0 = 14.92°$, $\alpha_l = 4.85°$, and $\hat{\omega} = 0.062$, whilst the fixed mesh zone is kept stationary and being remeshed using remeshing method. Spring based smoothing is used in the dynamic mesh scheme, zero damping coefficient is used in this analysis and indicates the damping value on the airfoil surface is zero [16]. The grid for airfoil has 84 nodes on the suction side and pressure side. The height of the first row of cells is set at a distance to the wall of 10^4c and this corresponds to $y^+ < 1$ to predict the phenomenon of laminar sub-layer accurately [14, 16]. The total number of meshes is of the order of 10^5. Simulation was performed in an open test region, the computational domain consists of two boundaries which are 16c and 12c away from the blade, respectively, see figure 4. The two boundaries have been placed sufficiently far away to eliminate their effect on the flow near the blade. The inlet and outlet boundaries are placed respectively 8c upstream and 45c downstream of the blade, making the uniform freestream velocity boundary condition at the inlet accurate enough and allowing a full development of the wake [14].

Results and Discussion

Numericalsimulation ofatwo-dimensional dynamicstallhas beendone using two turbulence model, namely *standard-kω* and *SST-kω* on the Boeing-Vertol V23010-1.58 rotorcraft airfoil. Experimental works and analytical model by Liiva [17] and Larsen [3] were used to validate numerical works in this paper. Figure 5 shows the comparison between lift coefficient which is produced using numerical simulation with those obtained from experiment and analytical works. In thecase ofα_0=14.92°, the liftcoefficientinfigure 5shows the effect ofoscillationsof theairfoilatthefullyattachedandseparatedflow. This isindicatedby the operation area inthiscaseis on theangle 10.34°<α <20.04°with thestaticstallpositionisatα ≈12.5°[17]. The results which is obtainedshowedsignificant differences byminimizingtime-step sizeup to0.001scomparedwith the largertimestepsizewhich is not presented in this paper. Accuracyofnumerical simulationshas significantly increasedcomparedwiththe use of largertimestepsize. The maximumpositionof theliftcoefficientthat indicatesthe occurrence ofdynamicstalliswell capturedusing thistimestepsize. Both of turbulence model, *standard-kω* and *SST-kω,* generateslift coefficient valueunderthe existing experimental resultand analytical model. Liftcoefficient which is produced by mathematicalmodelingconducted byLarsen[3] did notfluctuatein thestallarea, as well as with experimental resultsbyLiiva[17]. This phenomenon is different with numerical resultsthat generates high fluctuationinthehighangle of attack, the failureis may be due tothe 3D effectbecomesverysignificantcomparedto the lower angle of attack[18], therefore, both modelsfailpredict theliftcoefficientcorresponding with experimental data[14]. In general, the results ofnumerical simulations ofthestallareawould significantly different withthe experimental results, the results obtainedin the simulation tend to showdeepstall, similar resultswere also foundinWang'sstudy[14].

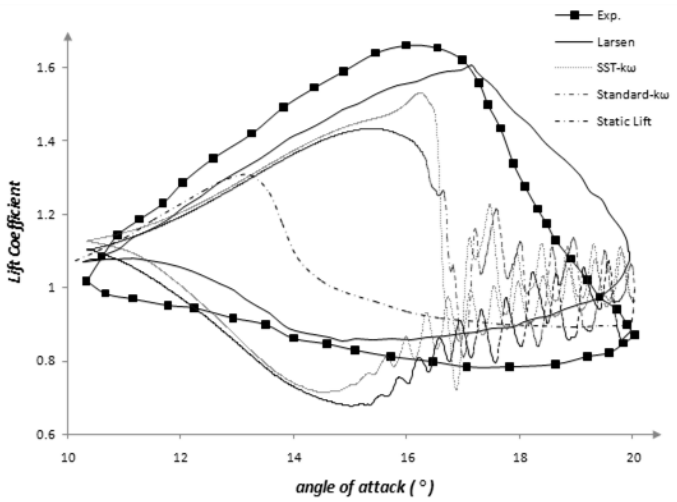

Figure 5. Dynamic lift coefficient between CFD and experimental and analytical works.

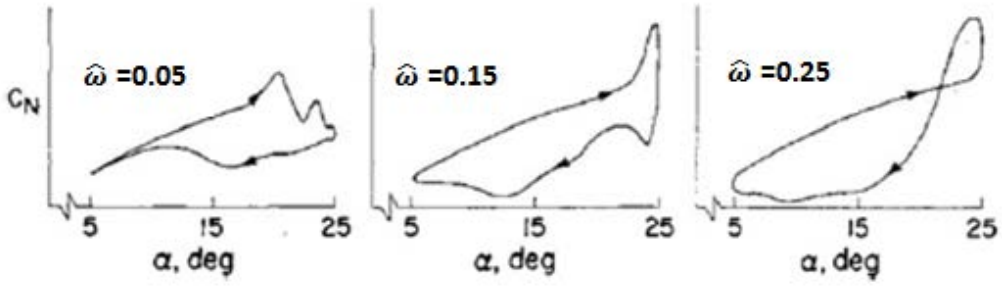

Figure 6. Comparison of the lift coefficient on different reduced frequency [21].

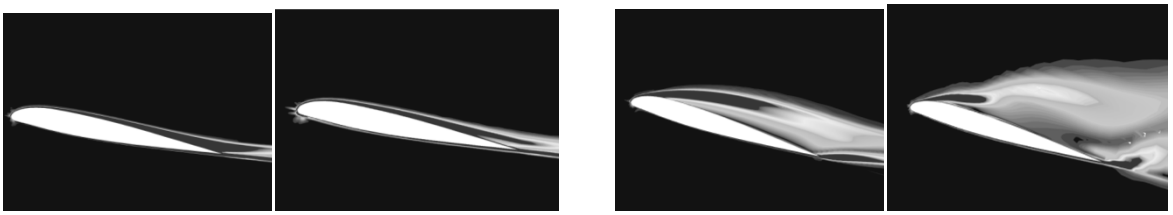

(a) *Dynamic*α = 10.34° (b) *Static*α = 10.34° (c) *Dynamic*α = 16.00°*ups.* (d) *Static*α = 16.00°

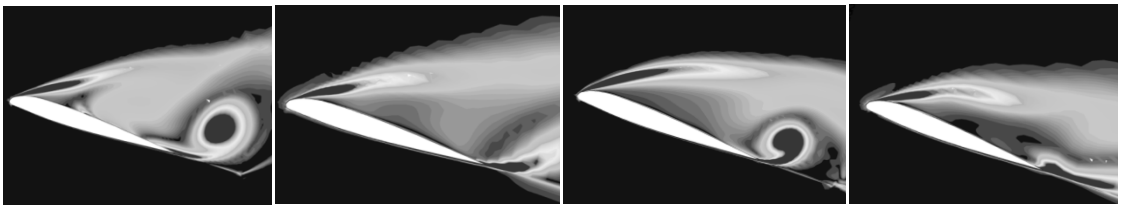

(e) *Dynamic*α = 17.00° *ups.* (f) *Static*α = 17.00° (g) *Dynamic* α = 20.04° (h) *Static*α = 20.04°

Figure 7. Vorticity field in dynamic and static conditions (1/s).

It is clearly seen thatthe *SST-kω*turbulence modelgenerate liftcoefficient data whichis moreaccurate than *standard-kω* model. Theposition of maximumliftcoefficient could not be well predicted using *standard-kω* turbulence model,and this model predict this location atα ≈15.5°by value1.43 compared with the experimental resultsat angle16.5°by value1.66.*SST-kω* turbulence model were able topredict themaximumpositionof the liftcoefficientatα ≈16.8by value 1.57, and this is much closer to the experimental data compared with the *standard-kω*. This isprobably due tothe *standard-kω* model is moredissipativein terms ofeddyenergyso that failed topredict the high adversepressuregradient on thecorrespondingangle[16, 17]. Liftcoefficient valueatthe highestangle of attack(α =20.04°) couldbe well predictedusing the*SST-kω*turbulencemodels, although atthelowestangle (α =10.34°), this value is still notwellpredictable. This might becauseof thecomputationalerrorbenumericallylargeenoughtosta gnationregion[19]. Unlike the case withthe *SST-kω*model, *standard-kω*modelfails topredict theliftcoefficient valueat the lowestangle of attackas well asthe highest angle. Similar results werealsoobtainedinthe studyWerneret. al. [20], where the use ofthe *SST-kω*model has a good performanceforlowandmediumangle of attack.

Lift coefficient decreasing at 16.8° < α < 20.04° indicates shedding phenomenon on the leading edge vortex, followed by formation of trailling edge vortex. Lift coefficient would increase again and this is the indication of the formation of leading edge vortex and followed by shedding of trailling edge vortex. This is explained by McCroskey [21], phase and value of the dynamic forces is depend on the value of reduced frequency $\hat{\omega}$. As the $\hat{\omega}$ increases, the position of the lift coefficient shifts to the higher angle of attack, or in other way, stall is delayed as illustrated on figure 6. In $\hat{\omega} = 0.05$, shedding of leading edge vortex occurs before the airfoil reach its maximum angle in upstroke phase, in $\hat{\omega} = 0.15$, the formation of secondary vortex is delayed to the downstroke phase, and in $\hat{\omega} = 0.25$, even the shedding of leading edge vortex occurs in the downstroke phase. Figure 5 shows that the position of the lift coefficient shifts to the right (On higher angle), followed by increasing of lift coefficient value, by the increase of $\hat{\omega}$ in range $0.05 < \hat{\omega} < 0.15$. By this explanation, it could be seen that this simulation has similar results with $\hat{\omega}$ = 0.05, agree with $\hat{\omega}$ = 0.062 that being used in present study.

Figure 7shows the comparison of vorticity patterns on thestaticanddynamicconditionsusing *SST-kω*turbulence model. Atα=10.34°, there is nosignificant differenceoccurredin bothstaticanddynamicconditions. It could be seen that thepattern offullyattachedflowoccurs inboththe simulation results, generating no differentliftcoefficient valueon the correspondingangle of attackisas shownin Figure5.Alongwith increasingangle of attack, there was a significant differenceinboth conditions,as shownin Figure7.cand7.d.Atangle 16.00°, the position ofstaticstallangle(α ≈12.5°)hasbeen passed, liftcoefficient valueofstatic condition has fallenandthere has been amassiveseparationon thesuctionside ofairfoil, while onthedynamiccondition,similar thingsdo nothappen. With increasingangle of attack, vortex formed on theleading edge, convected along suction side of airfoil, separated, andfollowed bytrailingedgevortexformationas shownin Figure7.e, and this isclearlydifferent from thestaticconditionat the corresponding angle. At an angle16.80°, liftcoefficientin thedynamicconditions achieves itsmaximumvalue, the further increase in angle of attackwillresult indecreasing ofliftcoefficientas shown infigure 5,characterized by trailingedgevortexformationat17.00°.

Development offluid flowphenomenaindynamicconditionshas beendiscussed inthis section. The results ofnumericalcomputationis able to capturequalitative datain the form oftravelingvortexphenomenathat characterizethe main features ofdynamicstall. Predictions which is obtainedcanprovidemore detailed informationon the development offluid flow onthe phenomenon ofdynamicstall.

Conclusion

In this study, two URANS turbulence model, namely *standard-kω*and *SST-kω* is usedtoperformnumericalsimulationsof fluid flow onan two-dimensionaloscillating airfoil. Bothturbulencemodelsunderpredicted theresultswhen it iscompared toexperimental data. *Standard-kω* looks too dissipative topredict theposition ofthe maximumliftcoefficient,which causesthe phenomenon ofdynamicstalloccursata lowerangleinthis model. More accurate results isdemonstrated bythe use ofthe SST-kω model, wherethe position of maximumliftcoefficientcan bepredicted better than *standard-kω*, exceptata highangle of attackwherethe 3D effectsbecomemoresignificant. The maincharacteristicsofdynamicstall, such asthe domination ofleading

edgevortexandliftcoefficienthysteresiscurvescan be capturedwellusingthis model. Nevertheless, the development of fluid flow phenomena of transition before and after the dynamic stall are less able to be accurately captured. In order toobtainmore detailedinformation, the useof more advancedCFDmethodssuch asLESandDESshould be made toaccommodatethe failure ofURANSin predictingthe flowphenomenainareaswitha highangle of attackdue tothe dominance of3D effects.

References

[1] Galvanetto, U., Piero, J., Chantharasenawong, C., 2008, An assessment of some effects of the nonsmoothness of leishman-beddoes dynamic stall model on the nonlinear dynamics of a typical aerofoil section. Journal of Fluid and Structures 24, 151-163.

[2] Witteveen, J.A.S., Sarkar, S., Bijl, H., 2007, Modeling physical uncertainties in dynamic stall induced fluid–structure interaction of turbine blades using arbitrary polynomial chaos. Computers and Structures 85, 866–878.

[3] Larsen, J.W., Nielsen, S.R.K., Krenk, S., 2007, Dynamic stall model for wind turbine airfoil. Journal of Fluid and Structures 23, 959-982.

[4] VISCWIND, 1999. Viscous effects on wind turbine blades, final report on the JOR3-CT95-0007, Joule III project, Technical Report ET-AFM-9902, Technical University of Denmark.

[5] Leishman, J.G., 2000. Principles of Helicopter Aerodynamics. Cambridge University Press, Cambridge.

[6] Hansen, M.H., Gaunaa, M., Madsen, H.A., 2004, A beddoes-leishman type dynamic stall model in state space and indical formulations. Risø National Laboratory Risø R-1354.

[7] Petot, D., 1989, Modélisation du décrochage dynamique. La Recherche Aérospatiale 5, 60-72.

[8] Gormont, R.E., 1973, A mathematical model of unsteady aerodynamics and radial flow for application to helicopter rotors. Technical Report TR 72-67, USAAV Labs.

[9] Johnson, W., 1970, The response and airloading of helicopter rotor blades due to dynamic stall. Massachusetts Institute of Technology ASRL TR 130-1.

[10] Øye, S., 1991, Dynamic stall simulated as time lag of separation. Technical Report, Department of Fluid Mechanics, Technical University of Denmark.

[11] Leishman, J.G., Beddoes, T.S., 1986a, A semi-empirical model for dynamic stall. Journal of the American Helicopter Society 34, 3–17.

[12] Leishman, J.G., Beddoes, T.S., 1986b, A generalised model for airfoil unsteady aerodynamic behaviour and dynamic stall using the indicial method. Proceedings of the 42nd Annual Forum of the American Helicopter Society.

[13] Meyer, M., Matthies, H.G., 2003, State-space representation of instationary two-dimentional airfoil aerodynamics. Journal of Wind Engineering and Industrial Aerodynamics 92, 263-274.

[14] Wang, S., Ingham, D. B., Ma, L., Pourkashanian, M., Tao, Z., 2010, Numerical investigations on dynamic stall of low Reynolds number flow around oscillating airfoils. Computers & Fluids 39, 1529–1541.

[15] Reu, T. and Ying, S. X., 1992, Hybrid grid approach to study dynamic stall. AIAA J. 30 (11), 2670-2676.

[16] Ansys F. Fluent user’s manual. Software release 13.

[17] Liiva, J., 1969. Unsteady aerodynamic and stall effects on helicopter rotor blade airfoil sections. Journal of Aircraft 6, 46–51.

[18] Raffel, M., Favier, D., Berton, E., Rondot, C., Nsimba, M., Geissler, W., 2006, Micro-PIV and ELDV wind tunnel investigations above a helicopter blade tip, Measur. Sci. Technol 17, 1652–1658.

[19] Perzon, S., Sjögren, T., and Jönson, A., 1998, Accuracy in computational aerodynamics part 2: base pressure, SAE Technical Paper.

[20] Wernert, P., Geissler, W., Raffel, M., Kompenhans J., 1996, Experimental and numerical investigations of dynamic stall on a pitching airfoil. AIAA J. 34 (5), 982–989.

[21] McCroskey, W., Carr, L., McAlister, K., 1976, Dynamic stall experiments onoscillating airfoils. AIAA J. 14 (1), 57–63.